MATRIX YIELDING ENERGY CONTRIBUTION TO FRACTURE TOUGHNESS OF PARTICLE REINFORCED COMPOSITES

Bernd Lauke

Leibniz-Institut für Polymerforschung Dresden e.V.Hohe Str. 6, 01069 Dresden, Germany
e-mail: laukeb@ipfdd.de

Keywords: Polymer-matrix composites, Fracture toughness, Modelling

Abstract
The incorporation of particles into polymer matrix causes local stresses in their neighbourhood when the composite is loaded. High multiaxial stress fields are created in front of a crack which leads to various fracture processes in a region close to the crack tip. One of these processes is matrix yielding around particles after their debonding The mechanical problem of a spherical particle within a spherical elastic/perfectly plastic matrix under uniform radial tensile stress was solved. Afterwards the yielding energy of the matrix shell was calculated. Finally an analytical equation for the composite fracture toughness for this mechanism was obtained, which is a function of mechanical properties of the components and particle volume fraction.

1. Introduction

Filled polymer composites have been studied extensively because of their technological and scientific importance. A survey of major results in this field was given in the review by Fu et al. [1]. The fracture toughness of particulate polymer composites shows a very complex variation with increasing particle fraction. Several studies found an increase of fracture toughness with incorporation of rigid particles into polypropylene such as, for example, Pukanszky [2]. Norman and Robertson [3] showed that the increase in fracture toughness arose almost completely from inelastic matrix deformation after particle debonding. Williams [4] considered among other mechanisms the debonding and the plastic void growth mechanisms after debonding of the particles from the matrix. Recently Zappalorto et al. [5] applied a similar approach for the calculation of void growth energy, extending it to the consideration of an interphase zone between particle and matrix. The present paper derives a model of composite crack resistance in itself by consideration of an energy density of matrix shells around debonded particles that depends on the position in front of the crack. This new consideration requires the integration of the energy density over the dissipation zone size. Because this direct integration causes problems in deriving an analytical equation of composite crack resistance, it was transformed into integration over the stress field which led finally to a new equation for composite crack resistance.

2. Crack resistance caused by matrix yielding

The composite energy release rate G (available from the change of the elastic energy and the applied load for an increment of crack growth) must at least be equal to the energy, R_c (crack resistance), necessary to initiate crack propagation: $G \geq G_c = R_c$ with G_c as fracture toughness of the composite (all these quantities as energy per unit area of crack growth, dA). The theoretical model may be explained by Fig. 1, where the cross sectional view of the zones ahead of a two-dimensional plane crack of area, A (unit thickness in the perpendicular z-direction), is sketched. The crack grows over a small area, dA. The particle position is given by cylindrical coordinates (ρ, φ, z) with the origin at the crack tip and z perpendicular to the plane.

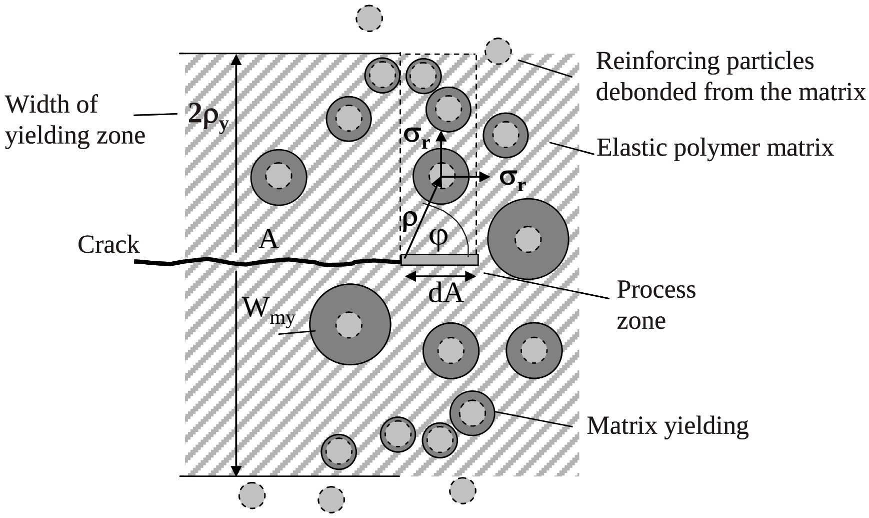

Figure 1. Cross sectional view of dissipation zone in front of the crack, with A: crack area, dA: crack extension, (ρ, φ, z): cylindrical coordinates of particle location (z perpendicular to the plane), W_{my}: matrix yielding energy around one particle.

During crack growth, the crack consumes energy, R_{pz}, to form the new fracture surface in the process zone. At the same time energy, R_{dz}, is dissipated within a larger zone of width, $2\rho_y$, by matrix yielding around debonded particles depicted as black circular shells while the remaining matrix behaves elastically, depicted as shaded area, cf. Fig. 1. The crack resistance can be calculated by:

$$R_c = R_{pz} + R_{dz} = R_m v_m + 2\int_0^{\rho_y} \eta_{my}(\rho)\, d\rho \qquad (2.1)$$

where η_{my} is the matrix yielding energy density, $R_m v_m$ is the process zone energy contribution, ρ is the distance coordinate from the crack tip and $2\rho_y$ is the width of dissipation zone in front of the crack, subsequently called the yielding zone.

The amount of dissipated energy, $\eta_{my}(\rho)$, and ρ_y were derived from the stress field around the crack tip on the basis of linear elastic fracture mechanics. The stress field is approximated by a uniform radial tensile stress, σ_0: $\sigma_0(\rho) = (\beta R_c E_c / \rho)^{1/2}$ where β, as a zone shape and size factor, can be used as a fitting parameter. This approximation neglects the differences in the values of the stresses. A similar approach was used by Zappalorto et al. [6], who argued that the hydrostatic stress component of the crack tip stress field is of major importance for such analysis. The half width of the dissipation zone, ρ_y, is thus given by:

$$\rho_y = \frac{\beta R_c E_c}{\sigma_{0,min}^{\;2}} \qquad (2.2)$$

with $\sigma_{0,min}$ defined below as a minimum radial stress where plastic yielding in the matrix shell around a particle starts. Details of the composite material are considered in the local heterogeneous structure. The volume specific yielding energy, η_{my}, was calculated by multiplying the particle density of the composite, n_p, by the yielding energy around one particle, $W_{my,}$ (see Fig. 1) as:

$$\eta_{my}(\rho) = n_p \; W_{my}(\rho) = \frac{3v}{4\pi r_p^3} \; W_{my}(\rho) \tag{2.3}$$

where r_p is the particle radius and v the particle volume fraction of the composite. After calculation of $W_{my}(\rho)$ the integral over the yielding zone width can be carried out. The integration over the distance, ρ, can be transformed into integration over the stress with the replacement: $d\rho = -2\beta R_c E_c (\sigma_0)^{-3} d\sigma_0$ as:

$$R_{dz} = 4\beta R_c E_c \int_{\sigma_{0,min}}^{\sigma_{0,max}} \eta_{my}(\sigma_0)\,(\sigma_0)^{-3} d\sigma_0 \tag{2.4}$$

with $\sigma_{0,min}$ as the minimum stress at which the yielding process starts in the matrix shell around the debonded particle and $\sigma_{0,max}$ where the whole matrix shell around one particle is yielding.

3. The mechanical problem

A spherical particle (index p) of radius r_p of elastic modulus, E_p, and Poisson's ratio, ν_p, within a spherical volume of matrix material (index m) of radius r_0 and elastic modulus, E_m, and Poisson's ratio, ν_m, was considered. This composite element is shown in Fig. 2 and possesses a local particle volume fraction of: $\tilde{v} = (r_p / r_0)^3$. The radius, r_0, describes the limit extension to ensure that the stress field of one particle does not interact with the stress field of others. At the outer surface, $r=r_0$, the composite volume element was loaded with the uniform radial tensile stress, $\sigma_0(\rho)$.

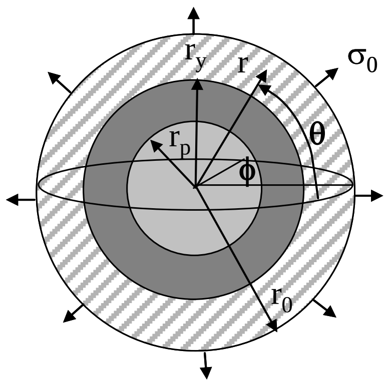

Figure 2. Geometrical model (called composite element) of a spherical particle of radius, r_p, embedded within a spherical matrix of radius, r_0, loaded by uniform tensile stress, σ_0. The radius, r_y, gives the transition between the yielding and elastic region of matrix.

The mechanical problem was described with spherical coordinates, r, θ, ϕ. After particle debonding, matrix yielding begins at the radius where the yield condition is first satisfied, which assumes that the maximum shear stress reaches a critical value (Tresca yield condition):

$$\sigma_\theta^{my} - \sigma_r^{my} = \sigma_{my} \qquad \text{with } \sigma_\theta^{my} > \sigma_r^{my} \qquad \text{and} \qquad \sigma_\theta^{my} = \sigma_\phi^{my} \tag{3.1}$$

where the index "my" indicates the matrix yielding region and σ_{my} is the matrix yield stress under uniaxial tension of an elastic/perfectly plastic matrix material.

3.1. Elastic solution, initiation of yielding

The loading situation as shown in Fig. 2 is considered for uniform tensile stresses for an intact particle/matrix interface and low enough to leave the matrix material in the elastic range. The equilibrium equations in curved coordinates for the stresses is given by the differential equation: $\frac{\partial \sigma_r}{\partial r} = \frac{2}{r}(\sigma_\theta - \sigma_r)$ and $\sigma_\theta = \sigma_\phi$ with $\sigma_r, \sigma_\theta, \sigma_\phi$ as normal, hoop and the circumferential stress, respectively.
Their solution is known as the Lamè solution:

$$\sigma_r = A_k + \frac{B_k}{r^3}, \sigma_\theta = A_k - \frac{B_k}{2r^3} \tag{3.2}$$

Inserting these solutions of stresses into the relations between deformations and displacements provides the radial displacement:

$$u = \frac{r}{E}\left[(1-2\nu)A_k - \frac{1+\nu}{2}\frac{B_k}{r^3}\right] \tag{3.3}$$

For the determination of the constants A and B within the particle (p) and the matrix (m), the following boundary conditions were used, at r=r_p: $\sigma_r^p = \sigma_r^m$, $u^p = u^m$, at r=r_0: $\sigma_r^m = \sigma_0$.The indices p and m indicate the stresses within particle and matrix, respectively. After solving these three linear equations for the constants A_p, A_m and B_m, the radial displacement and the stresses are obtained. The constant B_p is set to zero to avoid a stress singularity in the centre of the particle. After debonding, the matrix shell is under stress and may start yielding immediately after debonding. With the boundary conditions: $\sigma_r^m(r = r_p) = 0$ and $\sigma_r^m(r = r_0) = \sigma_0$ one obtains:

$$u_0 = u^m(r = r_0) = \frac{r_0}{E_m}\sigma_0 \frac{(1-2\nu_m) + \tilde{v}(1+\nu_m)/2}{1-\tilde{v}} = \frac{r_0}{E_m}\sigma_0 \tilde{C}_0 \tag{3.4}$$

With the yielding condition, Eq. (3.1), the solution of stresses provides the minimum uniform stress for initiation of matrix yielding:

$$s_{min} = \frac{\sigma_{0,min}}{\sigma_{my}} = \frac{2}{3}(1-\tilde{v}) \tag{3.5}$$

3.2. Matrix yielding

For uniform radial stresses, $\sigma_0 \geq \sigma_{0,min}$ matrix yielding starts over the matrix shell region. The stress equilibrium in this case takes the form: $\frac{\partial \sigma_r^{my}}{\partial r} = \frac{2}{r}\sigma_{my}$ with the solution:

$$\sigma_r^{my} = A_{my} + \sigma_{my} \ln(r/r_p)^2 \qquad (3.6)$$

with A_{my} as an integration constant, where the index "my" indicates the value within the yielding matrix shell.
To calculate the stress distribution over the whole matrix ($r_p \leq r \leq r_0$) with elastic and yielding behaviour and to determine the displacement, $u_{0,y}$, at $r=r_0$, the following boundary conditions for stresses are available, at r = r_p: $\sigma_r^{my} = 0$ at r = r_y: $\sigma_r^{my} = \sigma_r^m$ and $\sigma_\theta^{my} - \sigma_r^{my} = \sigma_{my}$ (yield condition) and at r = r_0: $\sigma_r^m = \sigma_0$.
With these four stress boundary conditions, the determination of the unknown stress constants: A_{my}, A_m, B_m and the position of the yielding region, $r=r_y$, was possible. The condition for the radial stress at $r=r_p$ provided a transcendental equation for the yield limit, r_y:

$$\ln(r_y/r_p) = \tilde{v}(r_y/r_p)^3/3 + s/2 - 1/3 \quad \text{with} \quad s = \sigma_0/\sigma_{my} \qquad (3.7)$$

The solution was fitted by a series up to the power of six as: $r_y(\nu_m, \tilde{v}, s)/r_p = \sum_n a_n s^n$ with (n=0..6). Finally, the total displacement at the outer surface $r=r_0$ was calculated using the constants, A_m, B_m, A_{my} and r_y:

$$u_{0,y} = u^m(r = r_0) = \frac{r_0}{E_m}\sigma_0\, \tilde{C}_{0,y}(s, \tilde{v}, \nu_m) = \frac{r_0}{E_m}\sigma_0\left[\frac{\tilde{v}}{s}\left(\frac{r_y(s)}{r_p}\right)^3(1-\nu_m) + 1 - 2\nu_m\right] \qquad (3.8)$$

4. Energy of plastic yielding, fracture toughness

The yielding energy is given by the product of applied force with corresponding displacement: $W_{my} = F_0\Delta u = 4\pi r_0^{\,2}\sigma_0\Delta u$. Elastic deformations and yielding are superimposed within the matrix. If the matrix shell were to be unloaded, the remaining displacement, Δu, is appropriate for the calculation of yielding energy. This is given approximately by: $\Delta u = u_{0,y} - u_0$ and:

$$\Delta u = \frac{r_0}{E_m}\sigma_0\Delta\tilde{C}(s, \tilde{v}, \nu_m) = \frac{r_0}{E_m}\sigma_0\left[\frac{1}{s}\tilde{v}(1-\nu_m)\left(\frac{r_y}{r_p}\right)^3 + (1-2\nu_m) - \frac{(1-2\nu_m) + \tilde{v}(1+\nu_m)/2}{1-\tilde{v}}\right] \qquad (4.1)$$

With this value, the yielding energy of the matrix shell around one debonded particle was calculated as:

$$W_{my} = 4\pi r_0^{\,2}\sigma_0\Delta u = 4\pi r_0^{\,3}\sigma_0^{\,2}\Delta\tilde{C}/E_m \qquad (4.2)$$

Inserting this into Eq. (2.3) leads to the volume density of yielding energy:

$$\eta_{my} = n_p\, W_{my} = \frac{3v}{4\pi r_p^{\,3}}\, W_{my} = \frac{3v}{\tilde{v} E_m}\sigma_0^{\,2}\, \Delta\tilde{C} \tag{4.3}$$

With this knowledge, the crack resistance caused by matrix yielding follows from Eq. (2.4) with the normalization $s = \sigma_0 / \sigma_{my}$:

$$R_{dz} = R_{my} = \frac{12\beta R_c E_c}{E_m} \frac{v}{\tilde{v}} \int_{s_{min}}^{s_{max}} \Delta\tilde{C}(s)\, (s)^{-1} ds \tag{4.4}$$

For the determination of the lower and upper bounds of integration, relation (3.7) was used. These bounds are important because they determine the amount of yielding energy. The lower limit, s_{min}, was obtained as the smallest stress for initiation of yielding at $r=r_y=r_p$ and is given by Eq. (3.5). For the determination of the upper bound that stress was determined at which the whole matrix region between $r_p \le r \le r_0$ yields, i. e. inserting $r_y=r_0$ in Eq. (3.7) and solving for s_{max}:

$$s_{max} = \sigma_{0,max} / \sigma_{my} = -2(\ln \tilde{v})/3 \tag{4.5}$$

For a local particle volume fraction, $\tilde{v}$, the yielding region is limited by $r_y = r_0 = r_p \tilde{v}^{-1/3}$. In the end, the composite crack resistance was obtained by inserting Eq. (4.4) into Eq. (2.1), with the result:

$$\frac{R_c}{R_m} = \frac{v_m}{1 - \dfrac{12\beta E_c}{E_m} \dfrac{v}{\tilde{v}} \displaystyle\int_{s_{min}}^{s_{max}} \Delta\tilde{C}(s)\, (s)^{-1} ds} \tag{4.6}$$

The matrix volume fraction in the crack plane was approximately evaluated by considering a cubic lattice particle arrangement. With a particle centre to centre distance of r_c one obtains: $v = (4\pi/3)(r_p/r_c)^3$ and consequently v_m is given by:

$v_m = 1 - \pi(r_p/r_c)^2 = 1 - \left(\frac{3}{4\pi}\right)^{2/3} \pi\, v^{2/3} \approx 1 - 1.21\, v^{2/3}$.

5. Discussion and conclusions

The proposed model is applied for glass-sphere-filled polyethylene with the following material properties for the spheres: elastic modulus E_p= 64 GPa and Poisson's ratio ν_p= 0.2. The elastic properties of the polyethylene matrix are: E_m= 520 MPa, ν_m= 0.35 and the matrix yield stress: $\sigma_{my} = 27\text{MPa}$. For the composite modulus the relation: $E_c = E_m \frac{(7+8v)(2+v)}{2(1-v)(7+4v)}$ proposed by Hashin and Shtrikman [7] was used.

The first goal was the calculation of the stress field and the radial displacement of the matrix shell. This generated the basis for calculating the yielding energy around one debonded particle. As long as the yield condition is not yet satisfied, the matrix behaves elastically. The radial and hoop stresses in the matrix shell after particle debonding are shown in Fig. 3 as functions of the normalized radial coordinate r/r_p for $s = s_{min}$; s_{min} is given in Eq. (3.5) and defines the loading case where yielding starts at the particle radius: $r_y = r_p$; i.e. the yield law Eq. (3.1) is just satisfied at this position. It was assumed that the particles are homogeneously distributed within the composite and that the local volume fraction corresponds to the particle volume fraction in the composite: $\tilde{v} = v$, i.e. the local composite element is representing the composite. Fracture toughness for the above given material properties is shown in Fig. 4.

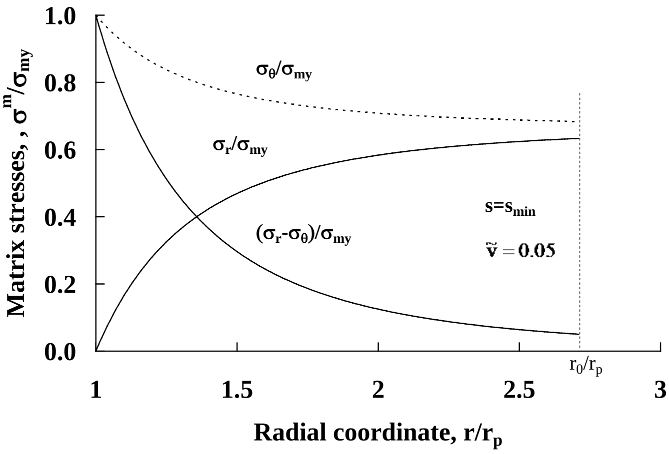

Figure 3. Distribution of radial (σ_r^m) and hoop (σ_θ^m) stresses within the matrix shell for the uniform stress: $s=s_{min}$ with $\tilde{v}=0.05$. Yielding condition Eq. (3.1) is satisfied at $r/r_p=1$.

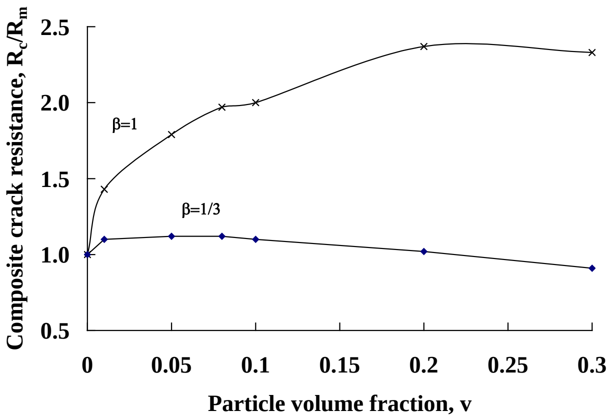

Figure 4. Normalized composite crack resistance (fracture toughness) as a function of particle volume fraction, influence of the shape factor, β.

The solution for two different values of the parameter β are compared. Composite crack resistance increases at first with increasing particle content and then reaches a plateau and for higher values starts to decrease. Such a qualitative behaviour was measured for many composites, cf. Refs. [2, 3, 8]. The interesting point is that the model is able to describe such a variation with v. This is caused by the superposition of different effects seen in Eq. (4.6) of R_c. The integrand, the prefactor and the integration limits are functions of the local particle volume fraction, $\tilde{v}$, whereas the prefactor also depends on v. The lower limit, s_{min}, decreases linearly with increasing $\tilde{v}$, but s_{max} drastically decreases with increasing $\tilde{v}$. Experimental results of glass spheres in a special thermoset reported by Norman and Robertson [3] show an increase of toughness with increasing particle volume fraction. The inelastic deformation of the matrix around debonded particles was considered as the most important contribution. Eq. (4.6) was applied for this case with the following material properties. For the glass spheres the same properties as given above were used. Thermoset matrix properties were given in Ref. [3] as: E_m= 2600 MPa, ν_m= 0.38, $\sigma_{my} = 110$ MPa and R_m=0.32 kJ/m^2. Theoretical and experimental results are compared in Fig. 5.

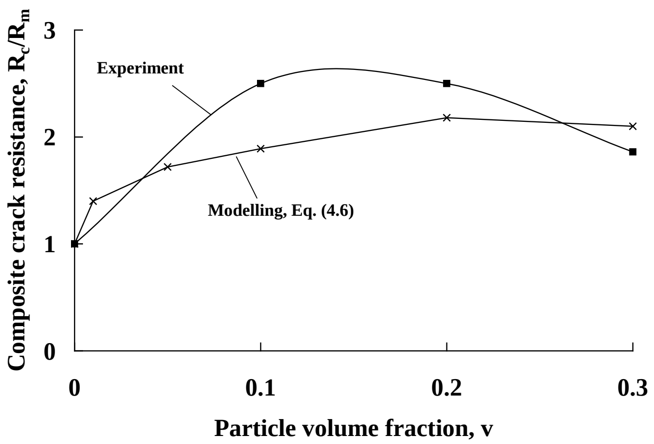

Figure 5. Experimental results for a glass sphere filled thermoset reported by Norman and Robertson [3] compared with the result of Eq. (4.6), $\beta = 1$.

The large underestimation for medium particle volume fractions might be a hint that matrix yielding after debonding is only one contribution.

References

[1] S. Y. Fu, X. Q. Feng, B. Lauke, Y. W. Mai. Effects of particle size, particle-matrix interface adhesion and particle loading on mechanical properties of particulate polymer composites. *Composites Part B* 39: 933-61, 2008.

[2] B. Pukanszky. Polypropylene: structure, blends and composites. In Karger-Kocsis J., *editor* , *Composites Vol. 3*, 1-70. Chapman & Hall, London, 1995.

[3] D. A. Norman, R. E. Robertson. Rigid-particle toughening of glassy polymers. *Polymer* 44: 2351-2362, 2003.

[4] G. Williams. Particle toughening of polymers by plastic void growth. *Composites Sci and Technology* 7:885-891, 2010.

[5] M. Zappalorto, M. Salviato, M. Quaresimin. Influence of the interphase zone on the nanoparticle debonding stress. *Comp. Sci. a. Technol*. 72: 49–55, 2011.

[6] M. Zappalorto, M. Salviato, M. Quaresimin. A multiscale model to describe nanocomposite fracture toughness enhancement by the plastic yielding of nanovoids, *Comp. Sci. a. Technol.* 72: 1683–1691, 2012.

[7] Z. Hashin and S. Shtrikman. On some variational principles in anisotropic and nonhomogeneous elasticity. *J. Mech. Phys. Solids* 10: 335-342, 1962.

[8] P. Dittanet and R. A. Pearson, Effect of silica nanoparticle size on toughening mechanisms of filled epoxy. *Polymer* 53:1890-1905, 2012.